A review of convolutional neural network-based computer-aided lung nodule detection system

Sekar Sari[1], Tole Sutikno[2], Indah Soesanti[1], Noor Akhmad Setiawan[1]
[1]Department of Electrical and Information Engineering, Faculty of Engineering, Universitas Gadjah Mada, Yogyakarta, Indonesia
[2]Department of Electrical Engineering, Faculty of Industrial Technology, Universitas Ahmad Dahlan, Yogyakarta, Indonesia

Article Info

ABSTRACT

Worldwide, lung cancer is the major cause of death and rapidly spreads. Lung tissue that is benign does not grow significantly, but lung tissue that is malignant grows rapidly and attacks the body, posing a grave threat to one's health. This paper provides a literature review of computer-aided detection (CAD) systems for lung cancer diagnosis. Preprocessing, segmentation, detection, and classification are the stages of the CAD system. This review divides the preprocessing into three stages: image smoothing, edge sharpening, and noise removal. Additionally, lung segmentation is divided into three stages: histogram-based thresholding, linked component analysis, and lung extraction. The detecting phase aids in decreasing the workload. Several techniques are briefly described, including random forest, naive bayes, k-nearest neighbor (k-NN), support vector machine (SVM), and convolutional neural network (CNN). Classification is the final stage; the image is then identified as containing or not possessing nodules. The prospect of incorporating CNN-based deep learning techniques into the CAD system is discussed. This paper is superior to other review studies on this topic due to its comprehensive examination of pertinent literature and structured presentation. We hope that our research may help professional researchers and radiologists design more effective CAD systems for lung cancer detection.

Corresponding Author:

Tole Sutikno
Department of Electrical Engineering, Faculty of Industrial Technology, Universitas Ahmad Dahlan
South Ringroad st., Tamanan, Banguntapan, Bantul, Special Region of Yogyakarta, Indonesia 55191
Email: tole@te.uad.ac.id

1. INTRODUCTION

Lung cancer is characterized by uncontrolled cell division in the lungs. Cells divide and replicate themselves. When damaged cells divide uncontrollably, they become tumors, which eventually hinder organs from functioning correctly. When compared to other kinds of cancer, lung cancer is by far the deadliest and most common form of the disease, making it the top cause of death globally [1]–[6]. Lung cancer is the world's second most common cancer, behind breast cancer. According to World Health Organization (WHO) figures issued in 2020, lung cancer mortality in Indonesia reached 28,633 in 2019. In 2022, the United States is expected to have 1,918,030 new cancer cases and 609,360 cancer deaths, with lung cancer, the leading cause of cancer death, accounting for approximately 350 deaths per day [7]. However, if nodules are found at an early stage, there is a chance that the human survival rate can be raised.

Lung cancer detection methods using computer-aided detection (CAD) have been developed in recent years [8]–[16]. Early identification of lung cancer has been shown to both lower mortality rates and increase the likelihood of survival. Nodules in the lungs that are still relatively tiny can be benign or malignant, depending on the circumstances, even if the nodules themselves are not cancerous. Lung tissue that is benign

does not experience much growth, however lung tissue that is malignant will develop swiftly and assault the body, making it extremely hazardous to one's health [17]. The most important goals of computer-aided design (CAD) are for reliably recognizing images and extracting regions of interest (ROI) from images obtained from a variety of imaging modalities. These imaging modalities include computed tomography (CT) scans, X-rays, position emission tomography (PET), and magnetic resonance imaging (MRI) [18]–[27]. CAD systems are further subdivided into computer-aided detection (commonly abbreviated as CADe) and computer-aided diagnosis (CADd) (CADx). The CADe system's capabilities are limited to identifying abnormal tissue regions and pictures, but the CADx system can be used to diagnose a disease by determining the sort of abnormality present and whether it is malignant [28].

Previously, a substantial amount of study was conducted on the examination of lung nodule identification using the CADe system. Because of limited resources and enormous volumes of data, this system is often based on traditional machine learning, as well as linear discriminant analysis, multiple gray-level thresholding, distance transformation, and support vector machines (SVM) [29]–[33]. However, in recent years, a number of researchers have created deep learning-based lung detection techniques. One of these ways is the convolutional neural network (CNN) approach, It has exceptional computer vision performance values, and increases the CADe system's accuracy and sensitivity [34]. Trends for the years 2019-2022 include deep learning in the form of CNN as well as the performance of each individual approach. The objective of this study is to give researchers with an overview of the CNN-based CAD system for the identification of lung nodules. The review will cover the phases of the CAD system for lung nodule identification in general, the preprocessing, the segmentation and detection techniques that have been extensively utilized from the beginning to the present, as well as the approach of lung nodule identification that is now being utilized.

2.   LUNG NODULES

Lung nodules are abnormal growths that develop within the lungs. Lung nodules are extremely frequent. The lung may have one or many nodules. Up to fifty percent of persons who have chest X-rays or CT scans possess them. Nodules can form in either lung. About 95% of lung nodules are benign (not cancerous). Infrequently, lung nodules indicate lung cancer. Because small lung nodules rarely cause symptoms, more testing are required to identify whether or not it is lung cancer.

Analysis of lung nodules is one of the stages that must be taken in order to successfully prevent lung cancer, which is accomplished through identification and categorization. Dark-level lung nodules are typically between 3 and 30 millimeters in diameter [34]. In general, these nodules have a diameter of around 3 millimeters. Figure 1 depicts samples of various types of lung nodule categories. The circumscribed, juxta vascular, juxta pleural, and pleural tails of nodules are represented in Figures 1(a) to 1(d), respectively. In contrast, juxta vascular nodules are firmly linked to blood vessels, while juxta pleural nodules are located in the region around the pleura [28]. Circumscribed nodules are not associated with any other tissue structures and are seen in a dispersed manner throughout the tissue.
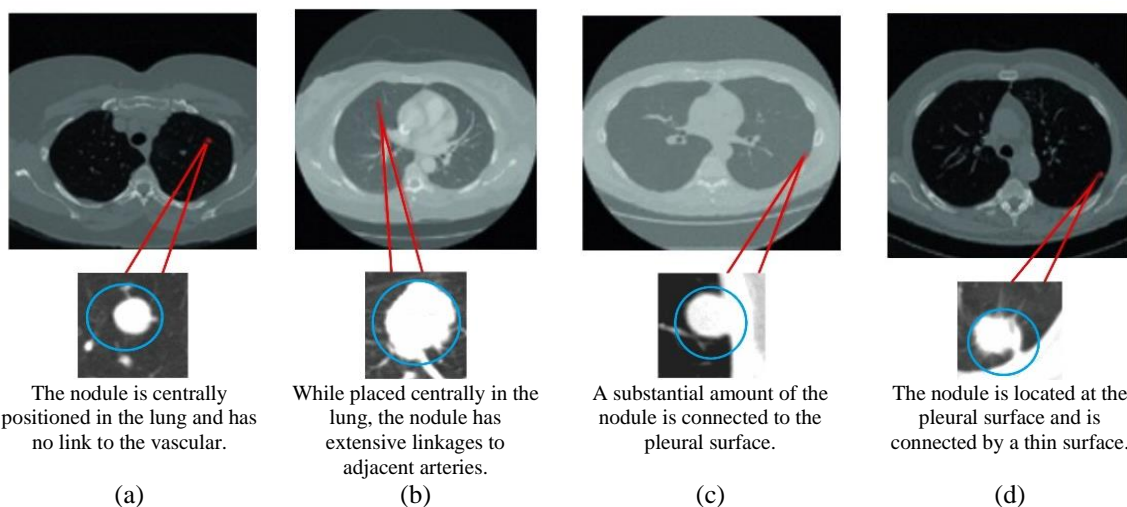

The nodule is centrally positioned in the lung and has no link to the vascular.	While placed centrally in the lung, the nodule has extensive linkages to adjacent arteries.	A substantial amount of the nodule is connected to the pleural surface.	The nodule is located at the pleural surface and is connected by a thin surface.
(a)	(b)	(c)	(d)

Figure 1. Categories of lung nodule samples [28], (a) well-circumscribed (b) juxta vascular, (c) juxta pleural, and (d) juxta pleural tail

3. COMPUTER-AIDED DESIGN FOR LUNG NODULE DETECTION

There are five stages to the computer-aided design (CAD) for the lung nodule detecting system, which are as follows: i) image acquisition, ii) preprocessing, iii) lung segmentation, iv) nodule detection, and v) classification. A comprehensive schematic representation of the lung CAD process is shown in Figure 2. Medical images are acquired by a variety of imaging modalities, including CT scans, X-rays, and MRI images [35]. Medical images can be gathered from publically available image databases to give researchers with a source of data for CADe system research, development, testing, evaluation, and benchmarking. Table 1 shows several databases of lung scans that are open to the public and can be used by anyone. These include Japanese society of radiological technology (JSRT), early lung cancer action program (ELCAP),
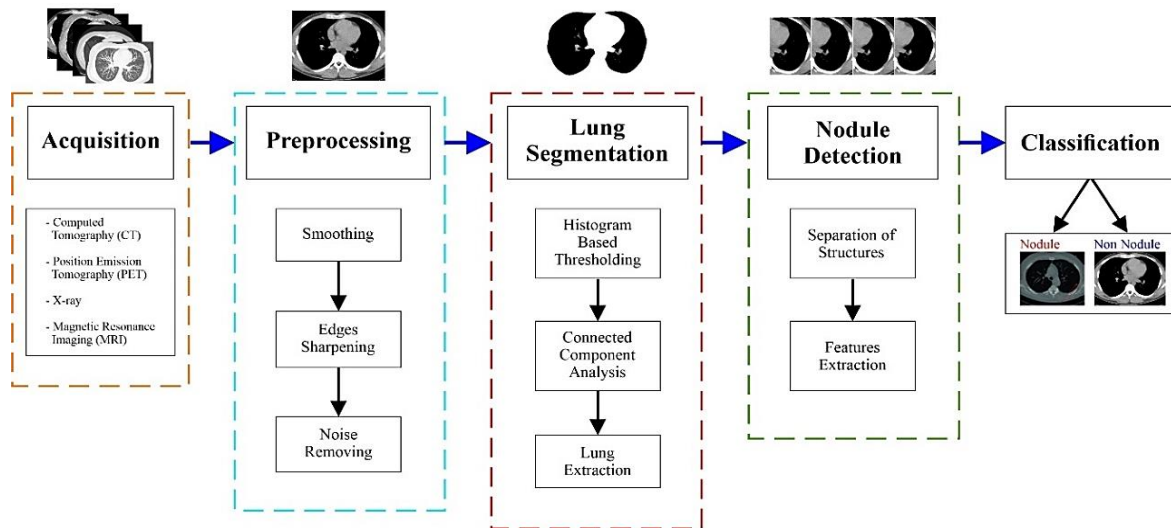

Figure 2. Acquisition, preprocessing, lung segmentation, nodule detection, and classification are the steps in the CAD schematic for lung nodule detection

Table 1. List of public lung image databases

Public Databases	Released Year	Scans	Modalities
PLCO Trial	1993	52,320	CXR
JSRT [36]	1998	247	CXR
ELCAP [37]	2003	50	CT
NELSON [38]	2003	15,822	CT
NELSON [39]	2003	15,822	CT
RIDER [40]	2004	48,698	CT
ANODE09 [41]	2009	55	CT
NLST Trial [42]	2009	75,000+	CT
Lung TIME [43]	2009	157	CT
LIDC–IDRI [1]	2011	1,018	CT, CR, DX
ILD [44]	2012	905	CT
ACRIN-NSCLC-FDG-PET [45]	2013	3,377	PT, CT, MR, CR, DX, SC, NM
NSCLC-Radiomics [46]	2014	1,265	CT, RTSTRUCT, SEG
LungCT-Diagnosis [47]	2015	61	CT
QIN Lung CT [48]	2015	47	CT
LISS [49]	2015	271	CT
LUNA 16/Ali Tianchi [50]	2016	888	CT
Italung-CT [51]	2016	122	CT
Kaggle Data Science Bowl [17]	2017	285,380	CT
UniToChest [52]	2021	306,440	CT

Note:
CXR: Chest X-Ray
CT: Computed Tomography
CR: Computed Radiography
DX: Digital X-ray
PT: Positron emission tomography (PET)
MR: Magnetic Resonance
SC: Secondary Capture
NM: Nuclear Medicine
RTSTRUCT: Radiotherapy Structure Set
SEG: Segmentation

JSRT: Japanese Society of Radiological Technology
ELCAP: Early Lung Cancer Action Project
NELSON: Nederlands Leuvens Longkanker Screeningsonderzoek
ANODE: Automatic Nodule Detection
LIDC: Lung Image Database Consortium
IDRI: Image Database Resource Initiative
ILD: Intersitial Lung Disease
LUNA: Lung Nodule Analysis
Italung-CT: Italian Lung

Cancer Screening Trial
PLCO: Prostate, Lung, Colorectal and Ovarian
NLST: National Lung Screening Trial
NELSON: Nederlands-Leuvens Longkanker Screenings Onderzoe

Dutch-Belgian randomized lung cancer screening trial or in Dutch *Nederlands–Leuvens Longkanker Screenings Onderzoek* (NELSON), automatic nodule detection 2009 (ANODE09), lung image database consortium and image database resource initiative (LIDC-IDRI), lung nodule analysis 2016 (LUNA16), Kaggle, and others. The lung ROI is segmented and noise is reduced during the preprocessing phase of the lung nodule CAD system. As a result, the prospecting range for lung nodules has been narrowed and the data have been normalized [10]. These include the weiner filter, the grayscale filter, the histogram equalization filter, the linear mapping filter, and the Gaussian lowpass filter [53], [54].

Lung segmentation is the process of separating a nodule from surrounding areas of a CT scan and then enhancing the resulting image to obtain more information about the nodule [55]. Accurate lung segmentation and a range of methods for obtaining lung volume from CT images are two indicators that reflect the efficiency of a system designed to identify lung nodules. Among them are quality thresholding, morphological procedures, the watershed approach, the active shape model (ASM), the active appearance model (AAM), and the faster region CNN (faster R-CNN) [50], [56].

The process of finding nodules in the lung that may progress to lung cancer is known as nodule detection [28]. Naive bayes, random forests, SVM's, multi-layer perception (MLP), and CNN's are some of the approaches used to identify lung nodules [1], [41], [57]. Because high sensitivity and poor accuracy values are frequently obtained during the nodule identification stage, a subsequent phase, termed false-positive reduction, is required [34]. The feature extraction method and nodule categorization with feature-based classifiers were engaged at this stage [41]. The form and texture are used to extract features. Shape qualities are measured using the geometric value of each structure (such as form proportion, density, roundness, elongation, weighted radial distance, and Boyce-Clark radial shape index); nodules are rounder than other tissue structures, thus look for the most spherical shape [58]. After the feature extraction step, use many supervised or unsupervised classifiers to detect the nodule and lower the FPs value [28]. In order to reduce the CADe system's false-positive rate, this FPs reduction stage focuses on recognizing true lung nodules from all suspected nodules and removing phony nodules. There will be four possible outcomes throughout the classifying procedure. A lung nodule that is correctly identified is referred to as a true positive (TP) or false negative (FN). If a lung nodule is identified wrongly, it is referred as as a "true negative" (TN) or "false positive" (FP) [59].

4. PREPROCESSING

Preprocessing is an essential first step in the CT images used for lung detection because the raw CT images contain a great deal of noise and extraneous data that will hinder the CAD system's ability to detect lung nodules [34]. This review divides preprocessing into three stages: image smoothing, edge sharpening, and noise removal. The preprocessing stages will be explained briefly in this section, and the section will conclude with the possibility of using CNN-based methods to remove noise from lung images.

4.1. Image smoothing

Images are impacted by a number of factors, not all of which are related to the viewer's ability to visually perceive the image. In addition to this, they make it more difficult to recognize and differentiate between image features that are important for various applications, such as pattern recognition and image segmentation. Noise is one of these factors that occurs quite frequently, and it has the potential to have a significant impact on both the visual quality of images and the performance of the majority of image processing tasks. It is due to inaccuracies that occurred during the image acquisition process [60].

Images are frequently captured despite the fact that the conditions are not optimal; for example, there may be insufficient light, excessive clarity, or unfavorable weather. The inability to acquire an image due to transmission errors, problems with networked cables, signal disturbances, problems with sensors, and so on can be caused by equipment of inferior quality. Therefore, the pixel intensity values do not accurately reflect the true colors that were captured during the real acquisition process. Because of these factors, a wide variety of techniques have been developed in order to retrieve lost image information and improve the details of images. Image smoothing is a technique that is included in preprocessing techniques and is used to remove possible image perturbations without losing any of the image's information [60]. Image smoothing is used to define smooth, consistent borders for segmented lungs near the mediastinum. As a result, smoothing operations must be restricted to the region around the mediastinum so that the contour of the lung in areas other than the mediastinum is not affected [61].

Some smoothing methods include restricted cubic splines (RCS), penalized splines (P-splines), natural splines (NS), and fractional polynomials (Fracpoly). The RCS is a cubic regression spline with continuous first and second derivatives at the knots for visual smoothness. RCS are further limited to be linear above the last knot and below the first. The linearity in the tails allows for a more compact model. P-splines were fitted using R's standard software implementation. By modeling the smooth function, P-splines provide an approach to

determining optimal smoothing via degrees of freedom that is relatively robust to the choice of location and a relatively large number of knots. The natural spline is simply a constrained cubic spline that employs B-spline basis functions instead of piecewise polynomials. Fractional polynomials, like P-splines and RCS, can be employed with any generalized linear model to analyze survival data. Although a global (rather than local) approach, the FP model has the advantage of being a simpler form than the other two possibilities and incorporating a wider range of functional forms than the normal polynomial family allows. A broader range of possible dose-response interactions could be accommodated [62], [63]. The mean filter, the Gaussian filter, anisotropic diffusion, the median filter, the adaptive median filter, conservative smoothing, and the alpha trim mean filter are other image smoothing methods that can be used to improve low-level distortion in lung images [37], [53]–[55], [58], [64].

4.2. Edges sharpening

Depending on the image domain, the sharpening methods can be divided into two groups: spatial-based and frequency-based methods. In the first scenario, we work directly with the pixel, whereas in the second, we work with the image's transform coefficients (Fourier or wavelet). Only when we recover the image using the inverse transform can we notice the effect of the alteration. The alteration of pixel values is the foundation of spatial domain techniques for sharpening images. Enhancing the contrast between various elements of the image is one method to make it better. There are various techniques for sharpening images in the spatial domain. Histogram equalization is one of the most well-known techniques (HE). Contrast stretching (CS), which is based on altering the dynamic range, or the range between the minimum and maximum intensity values of the image's gray levels, is another well-known method within the field of spatial domain sharpening. The simplest contrast stretch algorithm, linear contrast stretch (LCS), stretches the pixel values of a low- or high-contrast image by stretching the dynamic range across the entire image spectrum. This method's loss of certain details due to saturation and clipping is one of its drawbacks [1], [53], [55], [60], [65].

Frequency domain approaches rely on transformations such as the discrete Fourier (or cosine) transform or wavelet transforms. Each of these strategies is not unique; in fact, they are part of a family of methods that are fundamentally the same yet varies slightly from one another. They operate as follows: First, we apply one of these transformation methods; then, we process the changed image using one of these methods; and finally, the inverse transformation of the processed image yields the output. This method has a significant advantage: the ability to discern various parts in an image. Higher frequencies correspond to image edges or features, while lower frequencies belong to image smoothness. This simple split enables the image to be processed correctly depending on the aim. However, this also implies that we are processing details from multiple locations indistinguishably at the same time. This also occurs in smooth areas. In recent years, wavelet theory has emerged as a powerful image processing tool. This approach offers us with image spatial and frequency information. Adding high-pass or eliminating low-pass filtered versions from the image might improve the image. One of the early works on contrast sharpening in the wavelet domain was applying a parametrized hyperbolic function to the gradient of the wavelet coefficients. Since then, a great deal of work has been done in the wavelet domain. Loza *et al.*, for example, suggested a non-linear augmentation strategy based on the local dispersion of wavelet coefficients. This technique adaptively improves image contrast depending on local characteristics of the image's wavelet coefficients. A contrast enhancement technique based on scaling the internal noise of a dark image in the discrete cosine transform (DCT) domain. It is based on a physics concept known as "dynamic stochastic resonance" (DSR), which employs noise to increase the performance of a system [60].

The traits of smoothing and sharpening are diametrically opposite. As a result, there are few solutions to meet both goals concurrently, either jointly or independently. The first strategy is to process the image in two steps: first by performing one operation, and then by applying the second procedure on the produced image. The order in which we do the operations has a considerable influence on the result in this situation. Sharpening before smoothing may increase the significance of image noise, complicating the smoothing process. Smoothing before sharpening, on the other hand, risks losing information that the sharpening technique cannot recover. Although the second technique yields better outcomes in general, it is not the best option. As a result, in recent years, techniques capable of combining smoothing and sharpness have been presented [60]. The methods of smoothing and sharpening known as contrast limited adaptive histogram equalization (CLAHE) [66] and anisotropic filtering introduced by Perona and Malik (PM) [67] have been combined simultaneously by means of a synchronization algorithm, and the improvement in comparison to the corresponding two-step methods that are based on them can be seen here. The technique makes use of the benefits offered by these distinct models and combines them with the intention of developing a powerful instrument for the creation of medical images, more specifically for lung images.

4.3. Noise removing

Image denoising processes eliminate noise from images and restore them to their original state. How to discern between noise, edge, and texture is a fundamental issue in image denoising. Image denoising techniques are utilized in medical imaging, remote sensing, military surveillance, biometrics and forensics, industrial and agricultural automation, and individual recognition. Denoising algorithms are important pre-processing processes in medical and biomedical imaging that are used to remove medical noise such as speckle, Rician, quantum, and others [68].

The mean filter (MF), the adaptive mean filter (AMF), and the bilateral filter are three examples of the many algorithms that can be used to remove or reduce noise (BF). The mean filter (MF) is the simplest of the three, the AMF is a refinement of the mean filter, and the background subtraction filter (BF) is considered a state-of-the-art noise reduction technique. The BF compresses the filter range as well as the filter domain into a particular window size. The BF is a non-iterative adaptive smoothing filter that reduces noise while maintaining the edges of the objects contained within an image. The BF is comprised of three variables, which are as follows: the window size, the filter range, and the filter domain. Because of this, the camera is able to preserve a significant amount of the image's fine detail as well as its texture. However, the BF technique requires a considerable amount of computation and is mathematically complex; consequently, the development of a simple and quick algorithm for noise reduction that maintains excellent image quality would be very significant [69].

The majority of the filters listed above have generated results that are considered to be of a satisfactory quality; nonetheless, each of these filters has a few deficiencies. These disadvantages include insufficient test phase optimization, the need for manual parameter settings, and particular denoising models. The adaptability of CNN's has, fortunately, demonstrated that it is possible to overcome these shortcomings [70]–[73]. An overview of CNN's image denoising procedures is presented in Figure 3. It is intended that the explanations contained within this study will make it possible to comprehend the CNN architectures that are utilized in image denoising [68].
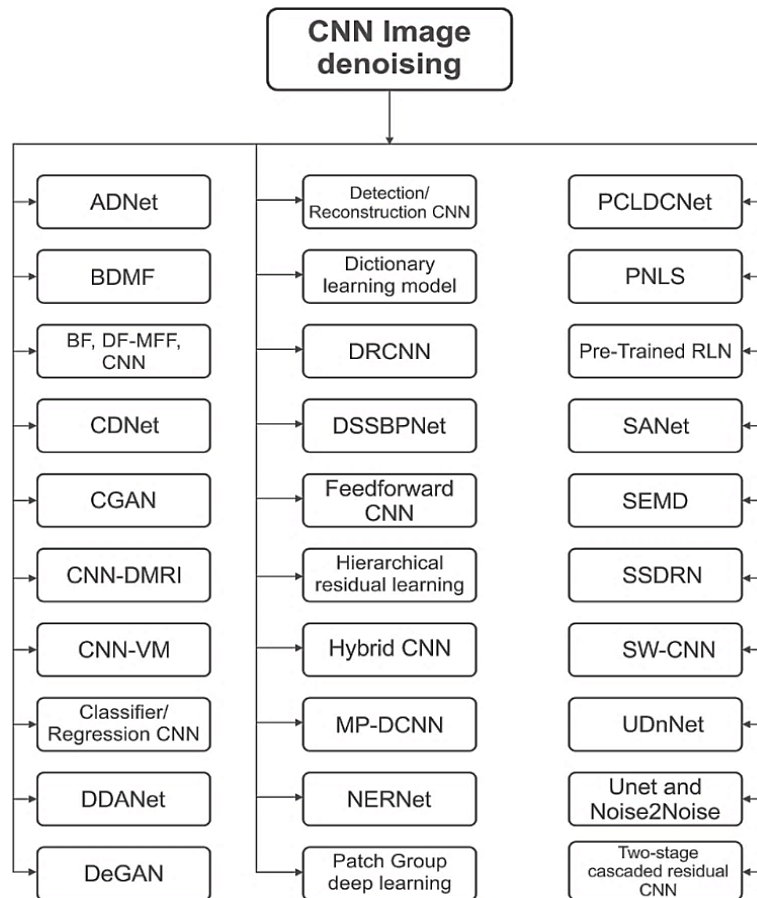

Figure 3. CNN-based methods for removing noise for lung images [68]

5. LUNG SEGMENTATION

Lung segmentation is a procedure that is used in lung detection. This process involves isolating lung nodules from other portions of the lung CT scan image and then further improving the image that is produced so that detail can be seen [55]. Lung segmentation techniques are broadly classified into four categories: i) deformable boundary-based techniques; ii) edge-based techniques; and iii) threshold-based techniques, and iv) registration-based method [28], [74]–[77]. Each of these categories has its own subcategories. Several of these methods of segmentation each have their own set of benefits and drawbacks. This review divides lung segmentation into three stages: histogram-based thresholding, connected component analysis, and lung extraction. The stages will be explained briefly in this section, and the section will conclude with the possibility of using CNN-based lung segmentation methods.

5.1. Histogram based thresholding

Because of its ease of use, the global histogram of a digital image is a popular tool for real-time image processing. It provides an important foundation for statistical techniques in image processing by giving a global description of the image's information. A pixel's color in a color image using RGB representation is a blend of the three primitive hues red, green, and blue. Each image pixel may be seen as a three-dimensional vector with three components representing the three colors of each image pixel. As a result, the global histograms representing the three primitive components may yield global information about the entire image. Histogram-based thresholding is a common segmentation approach that looks for peaks and troughs in the histogram. A standard segmentation strategy based on histogram analysis can only be carried out if the dominant peaks in the histogram can be accurately identified. Several frequently used peak-finding methods assessed the sharpness or area of the peak to determine the dominant peaks in the histogram. Although these peak-finding techniques are beneficial in histogram analysis, they may not always function effectively, especially when the image contains noise or radical change [78], [79].

In the research carried out by Filho *et al.* [58], the researchers decided to utilize a threshold value of 90 since they found that it was effective in the identification of lung nodules. The use of threshold approaches in lung segmentation helps make it simpler to locate nodules and reduces the amount of lung tissue that does not contain a nodule [1]. In the process of lung segmentation, in addition to thresholding techniques, there are also watershed techniques [54], morphological operations [65], active contour modeling (ACM) [56], active appearance modeling (AAM) [53], active shape modeling (ASM) [36], and fissure region segmentation [37]. Widodo *et al.* [53] came up with the idea for the AAM methodology, which is a statistical learning method that models parameters to characterize form differences across classes and variation in texture. In order to carry out the covariance matrix eigen analysis of the training vector in a way that is consistent with the shape and texture of the training image, the principal component analysis (PCA) is utilized. The AAM model as a whole is composed of three subcomponents, which are as follows: i) alignment of the shape data; ii) creation of a parameter model based on statistical and real data; and iii) template matching. The findings that were acquired from this segmentation were able to distinguish the lungs from the other tissues that were adjacent [53]. An active contour model was integrated with the field formulation of the locally biased image by using the ACM approach that was suggested by Kasinathan *et al.* [56] for the segmentation of lung tumors (ACM). In order to reconcile properly homogenous CT images and quickly split the tumor zone with an inhomogeneous intensity, the mean square error was utilized. The LIDC-IDRI database was utilized to test the suggested ACM approach, which is comprised of 850 images of the lesion and is able to reliably locate lung tumors in CT scans. The results of the testing were positive.

5.2. Connected component analysis (CCA)

Connected component analysis (CCA) also known as connected component labeling, blob extraction, or region labeling is a graph theory-based approach for determining the connectedness of "blob"-like regions in a binary image. Connected component analysis is frequently utilized in the same contexts as contours are used; however, connected component labeling can often provide more granular filtering of blobs in a binary image. The outline hierarchy is commonly a constraint when employing contour analysis (i.e., one contour contained within another). We can more readily segment and examine these structures with connected component analysis. The primary purpose of CCA is to extract related components in a binary image and synthetic data, such as area, bounding boxes, center of gravity, and so on, which will then be further processed based on the application. CCA is traditionally implemented as a mixture of two following computations: connected component labeling (CCL) and feature computation (FC). The CCL procedure distinguishes various connected components in the input binary image by assigning a unique label to all pixels that belong to the same connected component. The FC algorithm then creates these labeled images in order to obtain one or more of the above-mentioned synthetic data parameters required by the subsequent phases [80].

The labeled connected component in the binarized image is analyzed using connected component analysis. The pixels in the binary image are divided into multiple linked components based on their pixel connection. The lung lobes are segmented using the first-level linked components. The designated components' area and boundary information are utilized to determine the choice. The second level of linked components is identified, and geometric characteristics are retrieved from each component. The geometric characteristics used include area, bounding box, eccentricity, equivalent diameter, main axis length, minor axis length, and perimeter. The information gathered from the components is evaluated to identify whether or not they are tumors. An overall evaluation of lung nodules is provided in [81]. A lung nodule greater than 5 mm in size has a significant likelihood of becoming malignant cancer. According to their findings, an eccentric component with an overall size of 5 mm or greater is likely to be malignant. The findings of these tests are utilized to label the section as malignant and remove the remainder [82].

5.3. Lung extraction

The purpose of lung extraction is to identify the thoracic wall and mediastinum voxels, allowing the subsequent stages of work to focus entirely on the region that forms the lung parenchyma. This is accomplished once more through the use of the region-growing algorithm. Occasionally, the lung extraction stage incorrectly removes certain voxels from the pulmonary parenchyma. These errors can result in the exclusion of all potential nodules, resulting in a detection error. As a result, the rebuilding stage is critical for the preservation of peripheral nodules. In order to perform the reconstruction of the incorrectly eliminated lung outline, a previous knowledge about the object which is being segmented is used. The lung is a well-known organ with a gentle contour and no re-entrances. As a result, any hole or abrupt discontinuity observed on its outline is a clear indication of perimeter collapse and must be repaired [83].

Kuruvilla and Gunavathi [65] proposed a method for lung segmentation that makes use of morphological procedures on CT images. These operations are carried out by transforming grayscale images to binary images. The speed and user-friendliness of the morphological operation approach are two of its defining characteristics. Although Jayaraj and Sathiamoorthy [54] were the ones who initially introduced the watershed segmentation approaches, its most distinguishing feature is the capacity to isolate and identify items that are in close proximity to the image. This paradigm of mathematical morphology is built on the concept of regions. It is a kind of apparent image decomposition that assigns each pixel to a region or watershed. Deep learning, namely the faster convolutional neural network, was proposed by Huang *et al.* [50] as a method for performing the segmentation procedure for identifying lung CT images. It employs five layers of convolution at a rate that is lower than usual because to the improved resolution and increased segmentation precision it possesses. The suggested fully convolutional network (FCN) method was tested on the LIDC-IDRI database, and the results showed that it had an accuracy value of 94.6%. When separating CT images from the LIDC-IDRI database in 2018, Chunran and Yuanyuan [84] employed a FCN.

The regression neural network (RNN) segmentation approach was proposed by Messay *et al.* [85]. They developed a system that is completely automated (FA), a system that is semi-automated (SA), and a system that is hybrid. The FA and SA systems are what give rise to the hybrid system. These systems then yield many parameters, which are subsequently decided in an adaptive manner for each nodule by use of RNN. Additionally, the RNN method was presented by Sankar and George [86] in the year 2020. They are employing RNNs in an effort to enhance the identification of juxtapleural and juxtavascular lesions. Their suggested RNN technique performs better than the skeleton graph cut method and the level set method, which are both used to recognize lesions with the same intensity level. UNet and CNN are two approaches that were suggested by Shaziya and Shyamala [87] for segmenting lung CT images. According to the results of the dice similarity coefficient (DSC), the UNet approach is 1.27% more effective than CNN when it comes to image segmentation. In addition, Arora *et al.* [88] completed segmentation using a total of 662 chest X-ray (CXR) images using the UNet approach. When they segmented the lungs of TB patients, they found that the DSC value was 0.9680.

In point of fact, performance segmentation based on a rules-based approach is exactly the same as performance segmentation based on a data-based approach. Nevertheless, in order to train the learning model, a data-based method takes a significant amount of time, and the associated computational costs will be higher than those associated with a rule-based approach to CAD system optimization. In order to make researchers feel more at ease when using a rule-based approach to the processing of lung CT images, a rule-based approach can be accomplished by altering the manual settings of a data-based method [34]. As a consequence of this, the techniques of thresholding, FCN, RNN, and UNet are the most effective ways of segmentation for performing image detection tasks. For more details, the lung nodule preprocessing and segmentation techniques are shown in Table 2.

Table 2. Techniques for lung preprocessing and segmentation

Authors	Year	Databases	Scans	Nodules size	Preprocessing Methods	Segmentation methods
Kuruvilla and Gunavathi [65]	2014	LIDC-IDRI	155	260-400 mm	Gray scale to binary image	Morphological operations
De Carvalho Filho et al. [58]	2014	LIDC-IDRI	640	3 mm	Contrast, gaussian filter and median filter	Quality threshold clustering and region growing
Messay et al. [85]	2015	LIDC-IDRI	456	4.21-31.62 mm	A semi-automated (SA) system, a fully-automated (FA) system, and a hybrid system	RNN
Chen et al. [89]	2015	LIDC-IDRI	1010	8 mm	Resizing and Z-score normalization using mean and standard deviation	CNN and deep belief networks (DBN)
Widodo et al. [53]	2017	Private	120	0.5-10 mm	Histogram equalization and gaussian lowpass filter	AAM
Jiang et al. [1]	2018	LIDC-IDRI	1006	3 mm	Brighnest, position, shape, and repair of the lung contour for juxta-pleural nodules.	Local threshold segmentation
Chunran and Yuanyuan [84]	2018	LIDC-IDRI	1010	3-30 mm	Original images	FCN
Gong et al. [41]	2018	LUNA16 and ANODE09	1079	0.5–2 mm	OTSU thresholding	Segmentation of 3D levels and local image characteristics
Ausawalaithong et al. [90]	2018	JSRT, NIH	247 and 100	2048×2048 and 1024×1024 pixels	Increasing contrast, noise removal, image resizing and image normalizing	CNN
Anitha and Babu [37]	2019	LIDC and ELCAP	50 and 30	0.625 mm	Morphological transformation and weiner filter	Fissure regions segmentation
Kasinathan et al. [56]	2019	LIDC-IDRI	850	0.45-0.75 mm	Remove the mediastinum region and thoracic wall	ACM
Huang et al. [50]	2019	LIDC-IDRI and LUNA16	888	0.6-5.0 mm	Linear mapping	FCN
Ardila et al. [91]	2019	LIDC, LUNA, and NLST	1139	8–15 mm	CNN	CNN
Li et al. [36]	2020	JSRT	247	17.3 mm	Rib suppression	CNN
Sankar and George [86]	2020	LIDC-IDRI	1018	3 mm	Gaussian filtering	RNN
Shaziya and Shyamala [87]	2020	private	267	128×128 pixels	Data augmentasi are crop, zoom, rotate and flip	CNN and UNet
Arora et al. [88]	2021	NLM-China CXR	662	15 mm	CLAHE method	UNet++
Nazir et al. [92]	2021	LIDC-IDRI	4682	3–30 mm	Laplacian pyramid (LP) sparse vector fusion	CNN
Osadebey et al. [93]	2021	LIDC-IDRI	1100	3–30 mm	CNN	CNN
Chavan et al [94]	2022	Shenzhen and Montgomery	800	256×256	CNN	CNN
Tandon et al [95]	2022	LIDC-IDRI	1018	3 mm	Data augmentation methods (rescaling, rotation, horizontal and vertical flip)	CNN

6. LUNG NODULE DETECTION

The process of detecting objects in the lung tissue that are assumed to be nodules is referred to as "candidate nodule detection," which is also the name of the phrase. This detection stage is carried out after the lung segmentation stage. Lung segmentation is useful for lowering the burden of detecting CT input pictures because the background and undesired areas have been removed prior to this stage. It is possible to recognize lung nodules by the application of a number of distinct methods, such as random forest, SVM, naive bayes, k-nearest neighbor (k-NN), and CNN. The CNN system is comprised of several distinct designs, the most prominent of which are the CNN, a quicker R-CNN, a 3D CNN, and an R-CNN.

Using random forests and the 10-fold cross method, Gong et al. [41] were able to identify lung nodules for CAD systems. The created CAD system was validated using two datasets, specifically LUNA16 and ANODE09, respectively. Detection of lung nodules was carried out by De Carvalho Filho and colleagues using the SVM method. The SVM is a cutting-edge algorithm that is derived from the Vapnik-Chervonenkis theory.

The level of accuracy achieved by the SVM relies on the selection of kernel parameters such as C and the radial basis function (RBF). For the testing, the LIDC-IDRI database was utilized, and in total, 140 new exams were developed [58]. The Naive Bayes and KNN methods were proposed for the purpose of lung nodule detection by Nóbrega et al. [57]. The builder for these methods was based on a Gaussian distribution of the probability density function.

When attempting to detect lung nodules using machine learning techniques, the difficulty of defining and choosing the attributes of a certain image arises. As the number of photographs in each category rises, the process of extracting features from images gets increasingly time-consuming and labor-intensive [34] In addition, over the past few years, methods based on deep learning have been developed for the detection of lung nodules. The CNN method was developed by a group of researchers specifically for the purpose of detecting lung nodules. In its most basic form, a CNN is made up of three layers: a convolutional layer (CONV), a pooling layer, and a fully connected layer (FC). Jiang et al. [1] conducted research on the detection of lung nodules using the CNN method, modifying it to use the function of rectified linear units in place of the convolutional layer Rectified Linear Unit (ReLU). When compared to other activation functions on the CNN method, the process of error training is sped up by using ReLU, which is one of the advantages obtained from using it. At the pooling layer, operations known as max-pooling and average-pooling are carried out, whereas the FC layer is made up of four separate channels. assessment of the suggested CNN approach using the LIDC IDRI database. The CNN method, which consists of several layers, is utilized by Wang et al. [96] in their lung nodule detection process. The activation function of the convolution layer is Leaky ReLU, the pooling layer uses means and averages, and the final layer, the FC layer, uses global average pooling. The FC layer implements a feature mapping strategy that makes use of a 4 by 4 matrix kernel in an effort to cut down on the number of connected parameters. In addition, the batch normalization layer is implemented to lessen the impact of overfitting and speed up the convergence of the network [96]. Kasinathan et al. [56] and Li et al. [36] carried out yet another study for the purpose of detecting lung nodules using the CNN method. The CNN method is in the process of being developed, and it currently incorporates architectural models such as region-based fully convolutional networks (RFCN) [97], regional-CNN (R-CNN) [98], faster regional CNN (Faster R-CNN) [50], ResNet50 [57], and 3D-CNN [99].

Deep learning is crucial for enabling the CNN approach to be employed in the analysis of medical pictures as technology develops, the detection process gets computationally faster, and the amount of data accessible increases. This was made possible by the use of the CNN method. The CNN method has a number of benefits, the most notable of which are an enhanced image detection performance, high flexibility and adaptability to a wide variety of datasets, and the capacity to be designed automatically and effectively by making use of black-box operations [34]. According to the findings of previous research, the following are some advantages of deep learning:

− The performance of the CAD system in detecting nodules in lung cancer may be improved through the use of techniques from deep learning. Not only does the CAD system detect the presence of lung nodules, but it also provides information on the location of those nodules and has the ability to categorize detected nodules as either benign or malignant [97].
− Deep CNN has the potential to increase the sensitivity of the detection of lung nodules by reducing the value of FPs/scan, thereby lowering the error rate in detection and, of course, improving the quality of detection [99].
− Deep CNN can be used to detect lung nodules in a variety of dataset sources. For example, it can be used to detect data from hospital A, and then it can be used to detect data from hospital B. Deep CNN is able to discover various CT scans of the lungs and categorize them into distinct groups [37], [41], [50], [100].

7.   CLASSIFICATION: FALSE POSITIVE REDUCTION

Following the step of candidate nodule detection, the image is then further classified as either containing nodules or not containing nodules. This part of the process is referred to as the False Positive (FPs) reduction stage. The FPs reduction process can be broken down into two distinct categories: the first is the traditional feature-based classification, and the second is the CNN-based classification. In conventional feature-based classification, feature extraction and the detection of nodule candidate nodules are both utilized. There have been a few different approaches to feature extraction and candidate nodule detection that have been suggested. The following is a review of some of the publications that pertain to the aforementioned two classification stages for CAD systems in lung images.

The SVM method was proposed by Filho et al. [58] for the purpose of classifying lung images. This method utilizes data obtained from the LIDC-IDRI database as well as a feature extraction process that makes use of shapes and textures. With a FPs/scan value of 0.008 and a free-response operating characteristic (FROC) value of 0.8062, the findings indicated that the test had an accuracy of 97.55%, a sensitivity of 85.91%, and a

specificity of 97.70%. Additionally, the test had a sensitivity of 85.91%. Han *et al.* [101] and Boroczky *et al.* [102] carried out yet another investigation in which the SVM method was utilized. In this particular investigation, the classification performed by feature-based SVM was dependent on categorical rules. These categorical rules took the form of geometric or shape features, intensity features, gradient features, and eigenvalue-based features. The proposed system was tested on 205 patient cases taken from the openly accessible online LIDC database. The experimental results obtained a sensitivity of 89.2% at 4.14 FPs/scan, and the system was found to be successful [101]. The results of the study showed that the genetic algorithm method developed by Boroczky *et al.* for extracting features from private data obtained from lung CT scans (including 52 real nodules and 443 fake ones) was 100% accurate and 56.4% accurate [102].

Jia *et al.* [103] proposed several three-dimensional methods for lung detection, some of which are surface shadow display (SSD), volume rendering, maximum intensity rendering (MIP), and minimum intensity rendering (MIP) (VR). The process of feature extraction uses ROI to more accurately identify suspicious regions, paying particular attention to their shape, gray value, position, circularity, mean value of gray level, and smoothness. Also taken into consideration is the mean value of gray level. With a sensitivity of 95% on FPs/scan of 0.91, the proposed method was able to successfully detect lung image nodules. Tariq and Akram [55] investigated the use of the neurofuzzy method in the detection of lung nodules. The neurofuzzy classification can be broken down into two distinct sub-networks: the fuzzy self, which is responsible for managing the network, and the multilevel, multilayer perception (MLP). In order to generate a pre-classification vector, the feature vector is used as an input to the fuzzy layer. This pre-classification vector is then assigned to the MLP as a sample test classification. The fuzzy self-layer network is in charge of locating nodule pixels and organizing them into groups according to the similarity of the nodules (regardless of whether or not there are nodules), but with varying membership values. In addition to this, the MLP network will classify the input vectors that have been applied in order to select candidates from the appropriate category. The testing was done with a total of one hundred datasets of lung CT images taken from various patients. The accuracy reached using the strategy that was suggested is 95%. The back propagation neural network method, which is composed of three layers, was utilized by Talebpour *et al.* in the process of classifying nodules as distinct from other objects that are not nodules. There are 22 input neurons in the first layer, five hidden neurons in the second layer, and one neuron in the output layer of the third layer. The first layer is considered the input layer. Tan-sigmoid is an internal function that is present in every neuron. The proposed method was put to the test using the LIDC-IDRI database, and the results showed that it had a sensitivity of 90% on an FP/scan of 10 [104]. Kuruvilla and Gunavathi [65] carried out yet another study, this time making use of the back propagation neural network. The findings of the study indicated that a sensitivity of 91.4% could be achieved with an FP/scan value of 30.

A random forest method was proposed by Gong *et al.* [41] for the purpose of classifying lung nodules using the LUNA 16 and ANODE 09 databases. A sensitivity value of 79.3% was obtained from testing in both databases with an FP/scan value of 4, and a sensitivity value of 84.62% was obtained from testing with an FP/scan value of 2.8. Detecting lung cancer on CT images using the LIDC dataset was the focus of another study that was carried out by Jayaraj and Sathiamoorthy [54], which utilized the random forest method. The random forest method relies on a classification that takes into account both the index and the entropy to arrive at its conclusions. The results obtained using the proposed method had an accuracy of 89.90%, a sensitivity of 90.85%, and a specificity of 88.32%, respectively. Nobrega *et al.* [57] conducted research on the effectiveness of deep transfer learning when applied to the classification of lung nodule malignancy tasks. Their goal was to improve such systems and put them to the test using the LIDC database. The proposed method is a contrast between deep transfer learning and deep feature learning, and it yields the following results: an area under the curve (AUC) of 93.1%, a true positive rate (TPR) of 85.38%, an evaluation metrics accuracy (ACC) of 88.41%, precision of 73.48%, and an F1-score of 78.83%. They found that the deep transfer learning method is an effective way to take CT images of lung nodules and extract the most important features from those images. This was the finding of their research.

The CNN classification method is utilized next in the FPs reduction stage. Shin *et al.* [44] developed the CNN approach for lung nodule identification, an architecture created with GoogLeNet that comprises of a convolution layer, three pooling layers, and nine inception layers. GoogLeNet's inception layers are made up of six convolutional layers and one pooling layer. The system was tested using the ILD dataset, and the findings indicated a reduced accuracy (79%). To identify lung CT images, Golan *et al.* [105] suggested a deep CNN technique utilizing a back-propagation algorithm. CNN is divided into two segments. The first section comprises of numerous volumetric convolutions, rectified linear units (ReLU), and max-pooling layers. The second component is a classifier composed of many fully linked, threshold, and softmax layers. The system was tested using the LIDC dataset and yielded a poor sensitivity result of 78.9% at 20 frames per second. Anthimopoulos *et al.* devised and tested CNN for the categorization of ILD patterns. The suggested technique comprises of five convolutional layers, leaky ReLU activations, a pooling layer, and three dense layers. The

classification performance of lung patterns using the CNN approach is 85.5% [100]. Dou *et al.* proposed employing three-dimensional (3-D) CNN to improve automated lung nodule identification from volumetric CT data. The suggested approach was thoroughly tested in the LUNA16 challenge, yielding a sensitivity result of 90% with 8 FPs per scan [99]. Tekade and Rajeswari [17] presented lung cancer detection and classification using deep learning, and the technique is a 3D multipath VGG-like network that is tested on the LIDC, LUNA16, and Kaggle datasets. The result for lung nodule identification and classification is 95.60% accuracy and 0.387732 log loss. Kido *et al.* [98] developed a CAD method for lung anomalies based on CNN and areas with CNN properties (R-CNN). R-CNN is an object detection system that use a CNN to categorize picture areas inside an image. R-CNN was trained using marked aberrant lesions, and it indicated abnormal lesion bounding boxes on the test picture. Their proposed approach has an accuracy of 84.7%. Jiang *et al.* [1] suggested an automated detection approach for lung nodules based on a multigroup patch and a deep learning network. With 15.1 FPs per scan, the CAD system achieved a result sensitivity of 94%. Huang *et al.* [50] proposed utilizing deep convolutional neural networks to detect and separate lung nodules in thoracic CT images in a quick and fully automated manner. The accuracy gained at the false-positive (FP) reduction step, which is conducted using CNN, is 94.6% with 4 FPs per scan. The average dice coefficient of nodule segmentation compared to the ground truth is 0.793.

Lung nodule identification using multi-resolution convolutional networks was proposed by Li *et al.* [36] for the purpose of chest X-ray radiography. In order to extract the feature, they used patch-based multi-resolution convolutional networks, and for classification, they used four distinct fusion algorithms. They employed the JSRT database in order to evaluate their suggested technique. Within this database, they exhibited an accuracy of 99% while only using 0.2 FPs each scan. Kasinathan *et al.* [56] proposed utilizing CNN to automate the process of detecting and classifying three-dimensional lung tumors. The LIDC-IDRI dataset, which included 850 lung nodule-lesion pictures, was utilized in the evaluation of the suggested model. The outcome was that the model was accurate 97% of the time. In their study, Shi *et al.* [106] suggested a CNN multi-scale feature fusion approach for the identification of lung nodules. The framework for detection is made up of two parts: the production of region proposals and the minimization of false-positive results. The architecture of the CNN model is VGG16, and trials performed on the LUNA16 dataset demonstrate that it has an average sensitivity of 82.62%. Masood *et al.* suggested an automated technique for the identification of lung cancer by employing a method known as the improved multidimensional region-based fully convolutional network (mRFCN). The LIDC dataset was used to train and test their system, and the experiment findings demonstrate that their system has a sensitivity of 98.1% and an accuracy of 97.91% [97]. Wang *et al.* [96] proposed utilizing a raw patch-based CNN for the identification of lung nodules in CT images. On CT images taken from the LIDC-IDRI dataset, they evaluated the performance of ResNet in comparison to that of many alternative CNN architectures. As a result, they achieved a high detection sensitivity of 92.8% with 8 FPs per scan.

8.   CNN-BASED COMPUTER-AIDED LUNG NODULE DETECTION SYSTEM

It is abundantly evident that the CAD system is undergoing continuous development year after year based on the investigations and analyses that we have outlined above for the automatic CAD detection system. This takes place so that a higher-quality nodule detection may be achieved, which ultimately results in increased efficiency. When it comes to identifying and categorizing lung nodules, the most effective CAD system is one that is capable of achieving high levels of both accuracy and sensitivity. We conducted a literature review on lung nodule detection and summarized many articles that were published between 2006 and 2022 in the databases Science Direct, Springer Link, IEEE Xplore, and Web of Science. Our goal was to identify potential research areas and future problems. It is crucial to analyze the framework and assessment process of the technique that has been proposed, so it is not the primary focus while reviewing some of the most recent research, even if it is important to directly compare the outcomes of the studies. On the other hand, we assessed the technique of lung nodule identification in a CAD system based on the data that was utilized, the number of nodules, the image size, and the best performance, which included sensitivity and the reduction of false-positive results. In addition, we analyzed and evaluated a number of different techniques for detecting lung nodules at each stage, including preprocessing, segmentation, nodule identification, and classification between nodules and non-nodules using feature extraction and FPs reduction.

According to the findings of our review of the pertinent research literature, a number of studies examining the identification of lung nodules made use of a substantial number of datasets. CT scans are the most popular sort of dataset currently being used. Jiang *et al.* utilized the LIDC-IDRI dataset of 1006 images [1], Huang *et al.* used a total of 888 images [26], Kasinathan *et al.* used 850 images [56], Wang *et al.* [96], Masood *et al.* [97], and other researchers also used the same dataset. In addition to that, the LUNA16 dataset, which is utilized by a large number of people, is available. Gong *et al.* made use of the 1186-image LUNA16 dataset [41], which was previously utilized by Tekade *et al.* [17], Dou *et al.* [99], Shi *et al.* [106], and a number

of other researchers. Table 1 provides an overview of a variety of datasets taken from several different public databases, in addition to providing information on these datasets.

In addition to the dataset that was utilized, we also performed an analysis of the CAD system by employing the methods of preprocessing, segmentation, detection, and FPs reduction. The Table 2 provides a summary of some of the preprocessing and segmentation techniques that we use. The Gaussian filter and the Median Filter are the two types of preprocessing procedures that are utilized the most frequently. In order to analyze all 1018 photos that were taken from the LIDC-IDRI database, Jayaraj *et al.* utilized Gaussian and median filters. A gaussian filter is applied in order to reduce noise in lung cancer diagnosis, and a median filter is employed in order to remove salt and pepper noise, which is a type of very tiny noise that can be found in CT scans. In the CT picture of the lung, this will result in the smoothing of the image and a reduction in the speckle noise [54]. Widodo *et al.* [53], Filho *et al.* [58], and Sankar *et al.* [86] utilized the same method in their works.

The subsequent step in the process carried out by a CAD system is image segmentation. The process of distinguishing lung nodules from other sections of a CT scan picture of the lung and then enhancing the image that is produced as a consequence in order to acquire additional detail is referred to as lung segmentation. The thresholding method is one of the most used approaches to segmentation [1], [55], [58]. Deep learning as a segmentation approach has developed over time and can take on a variety of forms, depending on the lung imaging nodule being analyzed. Using a faster convolutional neural network, Huang *et al.* suggested a segmentation strategy for recognizing lung CT images [50], and they attained an accuracy of 94.6 f. RNN is a method that was proposed by Sankar and George [86] to enhance the identification of juxtapleural and juxtavascular lesions. UNet and CNN are two approaches that were proposed by Shaziya and colleagues for segmenting lung CT images. When it comes to picture segmentation, the findings of the Thedicee similarity coefficient (DSC) demonstrate that the UNet approach is 1.27 percent more effective than CNN [87]. In the TB category, Arora *et al.* performed segmentation with the help of the UNet, and as a result, they achieved a DSC value of 0.9680 [88]. As a direct consequence of this, deep learning segmentation strategies such as FCN, RNN, CNN, and UNet offer a great deal of promise.

The procedure of segmentation is followed by the identification of nodules and the extraction of features. The purpose of this step is to ascertain whether or not a certain picture is recognized as a nodule. Using SVM's and feature extraction with form and texture, Filho *et al.* [58] devised a method for the identification of nodules that was both highly accurate and sensitive. Tariq *et al.* [55] employ neurofuzzy to identify nodules, and they extract characteristics using vector and intensity. Back propagation neural network (BPNN) was utilized by Talebpour *et al.* for the purpose of detecting nodules, in conjunction with geometric and textural feature extraction [104]. However, machine learning algorithms for detecting nodules and extracting features have difficulty with the work of defining and selecting the characteristics of a particular picture, which also causes the task to become more time-consuming. In the process of nodule detection, deep learning CNNs are utilized extensively. Several studies, such as the ones by Jiang *et al.* [1] using CNN, Tekade *et al.* [17] using CNN with 3D multipath VGG, Wang *et al.* using CNN (ResNet) [96], and Masood *et al.* [97] using RFCN, Dou *et al.* [99] using 3D-CNN, have achieved an accuracy and sensitivity that is more than 90%. Performing methods like as feature extraction and false-positive reduction are essential for achieving the best results possible in lung nodule detection.

Moving forward, there is a pressing need for more study into the development of CAD systems for the identification of lung nodules. The target is to acquire a detection result that is more accurate as well as a high sensitivity value that has the potential to lower the value of FP reduction. The following is a list of significant concepts for potential CAD systems that can be utilized in the future to locate lung nodules:

− Developing new methods of deep learning, such as the CNN method, with the primary goal of enhancing the performance of lung nodule identification. In addition, the batch normalization layer can be included in order to lessen the effects of overfitting and speed up the convergence of the network [96].
− Developing a CAD system that is capable of detecting all types of lung nodules with high accuracy and sensitivity, as well as a low percentage of false-positive results while maintaining these characteristics.
− If the suggested technique is trained and evaluated using a large number of datasets, such as the LIDC-IDRI and LUNA16 public databases, then it will be able to provide a more comprehensive assessment of the general and clinical performance of the detection system.

9. CONCLUSION

In this study, we have presented a critical analysis of some of the research that has been done on CAD systems for lung nodule identification by doing literature investigations and analyzing the results. The research that has been done on CAD systems for lung nodule identification focuses on the identification of nodules in the lungs. There have been a few distinct lines of inquiry that have utilized CT scan photos to examine the

efficacy of the suggested method. After providing an overview of the computer-aided diagnosis (CAD) system for detecting lung nodules, it has been established that the system consists of various steps. These phases involve preparing or obtaining image data, preprocessing, segmenting, lung nodule detection, and FPs reduction, which incorporates feature extraction. Other steps include detecting and segmenting lung nodules. The steps are broken down into their component parts farther down in this article. We discovered that some of the works on lung nodule detection had better results than others based on parameters such as sensitivity, specificity, accuracy, and the number of FPs per scan, as well as other parameters, after reviewing a few of the most well-known works on the subject and evaluating the proposed method with a dataset taken from the LIDC-IDRI database. This was the conclusion we reached after looking at a few of the most well-known works on lung nodule detection and evaluating the method. In addition, we have provided an overview of the various methods that can be used for each of the steps of the process of identifying lung nodules. In recent years, deep learning algorithms such as CNN have been an increasingly popular means of locating prospective nodules and extracting attributes. Over the course of the last few years, this strategy has become increasingly common. Despite the fact that we discovered that some CAD systems achieved outstanding sensitivity with low false-positive rates, there are still a great many barriers to overcome in order to optimize CAD systems for the detection of lung cancer. It is expected that a capable CAD system will be able to assist radiologists in the detection of lung cancer. This is the single most critical thing that it ought to be able to accomplish.

ACKNOWLEDGMENT

REFERENCES

[1] H. Jiang, H. Ma, W. Qian, M. Gao, and Y. Li, "An automatic detection system of lung nodule based on multigroup patch-based deep learning network," *IEEE Journal of Biomedical and Health Informatics*, vol. 22, no. 4, pp. 1227–1237, 2018, doi: 10.1109/JBHI.2017.2725903.

[2] T. Uemura and T. Hida, "Durvalumab showed long and durable effects after chemoradiotherapy in stage III non-small cell lung cancer: Results of the PACIFIC study," *Journal of Thoracic Disease*, vol. 10, pp. S1108–S1112, 2018, doi: 10.21037/jtd.2018.03.180.

[3] T. Hou *et al.*, "Alpha thalassemia/intellectual disability X-linked deficiency sensitizes non-small cell lung cancer to immune checkpoint inhibitors," *Frontiers in Oncology*, vol. 10, 2020, doi: 10.3389/fonc.2020.608300.

[4] C. Olingy *et al.*, "CD33 expression on peripheral blood monocytes predicts efficacy of anti-PD-1 immunotherapy against non-small cell lung cancer," *Frontiers in Immunology*, vol. 13, 2022, doi: 10.3389/fimmu.2022.842653.

[5] M. Casás-Selves *et al.*, "Tankyrase and the canonical Wnt pathway protect lung cancer cells from EGFR inhibition," *Cancer Research*, vol. 72, no. 16, pp. 4154–4164, 2012, doi: 10.1158/0008-5472.CAN-11-2848.

[6] Z. Huang *et al.*, "Correlation of cancer stem cell markers and immune cell markers in resected non-small cell lung cancer," *Journal of Cancer*, vol. 8, no. 16, pp. 3190–3197, 2017, doi: 10.7150/jca.20172.

[7] R. L. Siegel, K. D. Miller, H. E. Fuchs, and A. Jemal, "Cancer statistics, 2022," *CA: A Cancer Journal for Clinicians*, vol. 72, no. 1, pp. 7–33, 2022, doi: 10.3322/caac.21708.

[8] M. S. AL-Huseiny and A. S. Sajit, "Transfer learning with GoogLeNet for detection of lung cancer," *Indonesian Journal of Electrical Engineering and Computer Science*, vol. 22, no. 2, pp. 470–478, 2020, doi: 10.11591/ijeecs.v22.i2.pp470-478.

[9] R. Pandian, D. N. S. Ravi Kumar, and R. R. Kumar, "Development of algorithm for identification of maligant growth in cancer using artificial neural network," *International Journal of Electrical and Computer Engineering*, vol. 10, no. 6, pp. 5709–5713, 2020, doi: 10.11591/ijece.v10i6.pp5709-5713.

[10] H. F. Kareem, M. S. AL-Husieny, F. Y. Mohsen, E. A. Khalil, and Z. S. Hassan, "Evaluation of SVM performance in the detection of lung cancer in marked CT scan dataset," *Indonesian Journal of Electrical Engineering and Computer Science*, vol. 21, no. 3, pp. 1731–1738, 2021, doi: 10.11591/ijeecs.v21.i3.pp1731-1738.

[11] R. D. Abdu-Aljabar and O. A. Awad, "Parallel extreme gradient boosting classifier for lung cancer detection," *Indonesian Journal of Electrical Engineering and Computer Science*, vol. 24, no. 3, pp. 1610–1617, 2021, doi: 10.11591/ijeecs.v24.i3.pp1610-1617.

[12] S. Kothari, S. Chiwhane, S. Jain, and M. Baghel, "Cancerous brain tumor detection using hybrid deep learning framework," *Indonesian Journal of Electrical Engineering and Computer Science*, vol. 26, no. 3, pp. 1651–1661, 2022, doi: 10.11591/ijeecs.v26.i3.pp1651-1661.

[13] O. R. Kadhim, H. J. Motlak, and K. K. Abdalla, "Computer-aided diagnostic system kinds and pulmonary nodule detection efficacy," *International Journal of Electrical and Computer Engineering*, vol. 12, no. 5, pp. 4734–4745, 2022, doi: 10.11591/ijece.v12i5.pp4734-4745.

[14] M. F. Abdullah, S. N. Sulaiman, M. K. Osman, N. K. A. Karim, S. Setumin, and I. S. Isa, "A new procedure for lung region segmentation from computed tomography images," *International Journal of Electrical and Computer Engineering*, vol. 12, no. 5, pp. 4978–4987, 2022, doi: 10.11591/ijece.v12i5.pp4978-4987.

[15] A. A. Abd Al-Ameer, G. A. Hussien, and H. A. Al Ameri, "Lung cancer detection using image processing and deep learning," *Indonesian Journal of Electrical Engineering and Computer Science*, vol. 28, no. 2, pp. 987–993, 2022, doi: 10.11591/ijeecs.v28.i2.pp987-993.

[16] R. S. Shankar, R. S. Chigurupati, P. Voosala, and N. Pilli, "An extensible framework for recurrent breast cancer prognosis using deep learning techniques," *Indonesian Journal of Electrical Engineering and Computer Science*, vol. 29, no. 2, pp. 931–941, 2023, doi: 10.11591/ijeecs.v29.i2.pp931-941.

[17] R. Tekade and K. Rajeswari, "Lung cancer detection and classification using deep learning," *Proceedings - 2018 4th International*

Conference on Computing, Communication Control and Automation, ICCUBEA 2018, 2018, doi: 10.1109/ICCUBEA.2018.8697352.

[18]   N. E. A. Khalid, M. F. Ismail, M. A. A. B. Manaf, A. F. A. Fadzil, and S. Ibrahim, "MRI brain tumor segmentation: A forthright image processing approach," *Bulletin of Electrical Engineering and Informatics*, vol. 9, no. 3, pp. 1024–1031, 2020, doi: 10.11591/eei.v9i3.2063.

[19]   I. Assini, A. Badri, A. Sahel, and A. Baghdad, "Hybrid multiple watermarking technique for securing medical images of modalities MRI, CT scan, and X-ray," *International Journal of Electrical and Computer Engineering*, vol. 10, no. 3, pp. 2349–2356, 2020, doi: 10.11591/ijece.v10i3.pp2349-2356.

[20]   N. Raju, H. B. Anita, and P. Augustine, "Identification of interstitial lung diseases using deep learning," *International Journal of Electrical and Computer Engineering*, vol. 10, no. 6, pp. 6283–6291, 2020, doi: 10.11591/IJECE.V10I6.PP6283-6291.

[21]   N. Saha and M. A. Rahaman, "Bone cancer detection using electrical impedance tomography," *Indonesian Journal of Electrical Engineering and Computer Science*, vol. 24, no. 1, pp. 245–252, 2021, doi: 10.11591/ijeecs.v24.i1.pp245-252.

[22]   R. Supriyanti, M. Alqaaf, Y. Ramadhani, and H. B. Widodo, "Morphological characteristics of X-ray thorax images of COVID-19 patients using the Bradley thresholding segmentation," *Indonesian Journal of Electrical Engineering and Computer Science*, vol. 24, no. 2, pp. 1074–1083, 2021, doi: 10.11591/ijeecs.v24.i2.pp1074-1083.

[23]   W. S. Alazawee, Z. H. Naji, and W. T. Ali, "Analyzing and detecting hemorrhagic and ischemic stroke-based on bit plane slicing and edge detection algorithms," *Indonesian Journal of Electrical Engineering and Computer Science*, vol. 25, no. 2, pp. 1003–1010, 2022, doi: 10.11591/ijeecs.v25.i2.pp1003-1010.

[24]   A. Elaraby and A. Taha, "An approach for cross-modality guided quality enhancement of liver image," *International Journal of Electrical and Computer Engineering*, vol. 12, no. 2, pp. 1449–1455, 2022, doi: 10.11591/ijece.v12i2.pp1449-1455.

[25]   H. A. Owida, H. S. Migdadi, O. S. M. Hemied, N. F. F. Alshdaifat, S. F. A. Abuowaida, and R. S. Alkhawaldeh, "Deep learning algorithms to improve COVID-19 classification based on CT images," *Bulletin of Electrical Engineering and Informatics*, vol. 11, no. 5, pp. 2876–2885, 2022, doi: 10.11591/eei.v11i5.3802.

[26]   V. Bhavana and H. K. Krishnappa, "Multi-modal image fusion using contourlet and wavelet transforms: a multi-resolution approach," *Indonesian Journal of Electrical Engineering and Computer Science*, vol. 28, no. 2, pp. 762–768, 2022, doi: 10.11591/ijeecs.v28.i2.pp762-768.

[27]   T. Asmaria, D. A. Mayasari, A. D. G. Febrananda, N. Nurul, A. J. Rahyussalim, and I. Kartika, "Computed tomography image analysis for Indonesian total hip arthroplasty designs," *International Journal of Electrical and Computer Engineering*, vol. 12, no. 6, pp. 6123–6131, 2022, doi: 10.11591/ijece.v12i6.pp6123-6131.

[28]   F. Shaukat, G. Raja, and A. F. Frangi, "Computer-aided detection of lung nodules: A review," *Journal of Medical Imaging*, vol. 6, no. 02, p. 1, 2019, doi: 10.1117/1.jmi.6.2.020901.

[29]   S. Saeed and A. Abdullah, "Recognition of brain cancer and cerebrospinal fluid due to the usage of different MRI image by utilizing support vector machine," *Bulletin of Electrical Engineering and Informatics*, vol. 9, no. 2, pp. 619–625, 2020, doi: 10.11591/eei.v9i2.1869.

[30]   S. Hartini and Z. Rustam, "The comparison study of kernel KC-means and support vector machines for classifying schizophrenia," *Telkomnika (Telecommunication Computing Electronics and Control)*, vol. 18, no. 3, pp. 1643–1649, 2020, doi: 10.12928/TELKOMNIKA.v18i3.14847.

[31]   S. A. Taie and W. Ghonaim, "A new model for early diagnosis of alzheimer's disease based on bat-SVM classifier," *Bulletin of Electrical Engineering and Informatics*, vol. 10, no. 2, pp. 759–766, 2021, doi: 10.11591/eei.v10i2.2714.

[32]   O. Y. Ogundepo, I. O. A. Omeiza, and J. P. Oguntoye, "Optimized textural features for mass classification in digital mammography using a weighted average gravitational search algorithm," *International Journal of Electrical and Computer Engineering*, vol. 12, no. 5, pp. 5001–5013, 2022, doi: 10.11591/ijece.v12i5.pp5001-5013.

[33]   B. S. Shukur and M. M. Mijwil, "Involving machine learning techniques in heart disease diagnosis: a performance analysis," *International Journal of Electrical and Computer Engineering*, vol. 13, no. 2, pp. 2177–2185, 2023, doi: 10.11591/ijece.v13i2.pp2177-2185.

[34]   W. Cao, R. Wu, G. Cao, and Z. He, "A comprehensive review of computer-aided diagnosis of pulmonary nodules based on computed tomography scans," *IEEE Access*, vol. 8, pp. 154007–154023, 2020, doi: 10.1109/ACCESS.2020.3018666.

[35]   V. A. Binson and M. Subramoniam, "Advances in early lung cancer detection: A systematic review," *2018 International Conference on Circuits and Systems in Digital Enterprise Technology, ICCSDET 2018*, 2018, doi: 10.1109/ICCSDET.2018.8821188.

[36]   X. Li *et al.*, "Multi-resolution convolutional networks for chest X-ray radiograph based lung nodule detection," *Artificial Intelligence in Medicine*, vol. 103, 2020, doi: 10.1016/j.artmed.2019.101744.

[37]   S. Anitha and T. R. Ganesh Babu, "An efficient method for the detection of oblique fissures from computed tomography images of lungs," *Journal of Medical Systems*, vol. 43, no. 8, 2019, doi: 10.1007/s10916-019-1396-0.

[38]   S. G. Armato *et al.*, "The lung image database consortium (LIDC) and image database resource initiative (IDRI): A completed reference database of lung nodules on CT scans," *Medical Physics*, vol. 38, no. 2, pp. 915–931, 2011, doi: 10.1118/1.3528204.

[39]   Y. R. Zhao, X. Xie, H. J. De Koning, W. P. Mali, R. Vliegenthart, and M. Oudkerk, "NELSON lung cancer screening study," *Cancer Imaging*, vol. 11, no. SPEC. ISS. A, 2011, doi: 10.1102/1470-7330.2011.9020.

[40]   S. G. Armato *et al.*, "The reference image database to evaluate response to therapy in lung cancer (RIDER) project: A resource for the development of change-analysis software," *Clinical Pharmacology and Therapeutics*, vol. 84, no. 4, pp. 448–456, 2008, doi: 10.1038/clpt.2008.161.

[41]   J. Gong, J. yu Liu, L. jia Wang, X. wen Sun, B. Zheng, and S. dong Nie, "Automatic detection of pulmonary nodules in CT images by incorporating 3D tensor filtering with local image feature analysis," *Physica Medica*, vol. 46, pp. 124–133, 2018, doi: 10.1016/j.ejmp.2018.01.019.

[42]   "NLST datasets," [Online]. Available: https://cdas.cancer.gov/nlst/.

[43]   M. Dolejsi, J. Kybic, M. Polovincak, and S. Tuma, "The lung TIME: Annotated lung nodule dataset and nodule detection framework," *Medical Imaging 2009: Computer-Aided Diagnosis*, vol. 7260, p. 72601U, 2009, doi: 10.1117/12.811645.

[44]   H. C. Shin *et al.*, "Deep convolutional neural networks for computer-aided detection: CNN architectures, dataset characteristics and transfer learning," *IEEE Transactions on Medical Imaging*, vol. 35, no. 5, pp. 1285–1298, 2016, doi: 10.1109/TMI.2016.2528162.

[45]   L. Kinahan, P. Muzi, M. Bialecki, B. Herman, and B. Coombs, "Data from the ACRIN 6668 trial NSCLC-FDG-PET [Data set]. The cancer imaging archive," 2019, doi: 10.7937/tcia.2019.30il.

[46]   M. Hershman *et al.*, "Impact of interobserver variability in manual segmentation of non-small cell lung cancer (Nsclc) applying low-rank radiomic representation on computed tomography," *Cancers*, vol. 13, no. 23, 2021, doi: 10.3390/cancers13235985.

[47]   O. Grove *et al.*, "Quantitative computed tomographic descriptors associate tumor shape complexity and intratumor heterogeneity with prognosis in lung adenocarcinoma," *PLOS ONE*, vol. 10, no. 3, p. e0118261, Mar. 2015, doi: 10.1371/journal.pone.0118261.

[48] K. Smith, "QIN LUNG CT."

[49] G. Han *et al.*, "The LISS - A public database of common imaging signs of lung diseases for computer-aided detection and diagnosis research and medical education," *IEEE Transactions on Biomedical Engineering*, vol. 62, no. 2, pp. 648–656, 2015, doi: 10.1109/TBME.2014.2363131.

[50] X. Huang, W. Sun, T. L. (Bill) Tseng, C. Li, and W. Qian, "Fast and fully-automated detection and segmentation of pulmonary nodules in thoracic CT scans using deep convolutional neural networks," *Computerized Medical Imaging and Graphics*, vol. 74, pp. 25–36, 2019, doi: 10.1016/j.compmedimag.2019.02.003.

[51] S. Diciotti, G. Picozzi, M. Falchini, M. Mascalchi, N. Villari, and G. Valli, "3-D segmentation algorithm of small lung nodules in spiral CT images," *IEEE Transactions on Information Technology in Biomedicine*, vol. 12, no. 1, pp. 7–19, 2008, doi: 10.1109/TITB.2007.899504.

[52] H. A. H. Chaudhry *et al.*, "UniToChest: A lung image dataset for segmentation of cancerous nodules on CT scans," *Lecture Notes in Computer Science (including subseries Lecture Notes in Artificial Intelligence and Lecture Notes in Bioinformatics)*, vol. 13231 LNCS, pp. 185–196, 2022, doi: 10.1007/978-3-031-06427-2_16.

[53] S. Widodo, R. N. Rohmah, and B. Handaga, "Classification of lung nodules and arteries in computed tomography scan image using principle component analysis," *Proceedings - 2017 2nd International Conferences on Information Technology, Information Systems and Electrical Engineering, ICITISEE 2017*, vol. 2018-January, pp. 153–158, 2018, doi: 10.1109/ICITISEE.2017.8285485.

[54] D. Jayaraj and S. Sathiamoorthy, "Random forest based classification model for lung cancer prediction on computer tomography images," *Proceedings of the 2nd International Conference on Smart Systems and Inventive Technology, ICSSIT 2019*, pp. 100–104, 2019, doi: 10.1109/ICSSIT46314.2019.8987772.

[55] A. Tariq and M. U. Akram, "Lung nodule detection in CT images using neuro fuzzy classifier," *Telkomnika*, vol. 11, no. 2, pp. 331–336, 2013, doi: 10.12928/telkomnika.v11i2.934.

[56] G. Kasinathan, S. Jayakumar, A. H. Gandomi, M. Ramachandran, S. J. Fong, and R. Patan, "Automated 3-D lung tumor detection and classification by an active contour model and CNN classifier," *Expert Systems with Applications*, vol. 134, pp. 112–119, 2019, doi: 10.1016/j.eswa.2019.05.041.

[57] R. V. M. da Nóbrega, P. P. Rebouças Filho, M. B. Rodrigues, S. P. P. da Silva, C. M. J. M. Dourado Júnior, and V. H. C. de Albuquerque, "Lung nodule malignancy classification in chest computed tomography images using transfer learning and convolutional neural networks," *Neural Computing and Applications*, vol. 32, no. 15, pp. 11065–11082, 2020, doi: 10.1007/s00521-018-3895-1.

[58] A. O. De Carvalho Filho, W. B. De Sampaio, A. C. Silva, A. C. de Paiva, R. A. Nunes, and M. Gattass, "Automatic detection of solitary lung nodules using quality threshold clustering, genetic algorithm and diversity index," *Artificial Intelligence in Medicine*, vol. 60, no. 3, pp. 165–177, 2014, doi: 10.1016/j.artmed.2013.11.002.

[59] G. Zhang *et al.*, "Automatic nodule detection for lung cancer in CT images: A review," *Computers in Biology and Medicine*, vol. 103, pp. 287–300, 2018, doi: 10.1016/j.compbiomed.2018.10.033.

[60] C. Pérez-Benito, S. Morillas, C. Jordán, and J. A. Conejero, "Smoothing Vs. sharpening of colour images: Together or separated," *Applied Mathematics and Nonlinear Sciences*, vol. 2, no. 1, pp. 299–316, 2017, doi: 10.21042/amns.2017.1.00025.

[61] S. Ukil and J. M. Reinhardt, "Smoothing lung segmentation surfaces in three-dimensional X-ray CT images using anatomic guidance," *Academic Radiology*, vol. 12, no. 12, pp. 1502–1511, 2005, doi: 10.1016/j.acra.2005.08.008.

[62] U. S. Govindarajulu, D. Spiegelman, S. W. Thurston, B. Ganguli, and E. A. Eisen, "Comparing smoothing techniques in Cox models for exposure-response relationships," *Statistics in Medicine*, vol. 26, no. 20, pp. 3735–3752, 2007, doi: 10.1002/sim.2848.

[63] U. S. Govindarajulu, E. J. Malloy, B. Ganguli, D. Spiegelman, and E. A. Eisen, "The comparison of alternative smoothing methods for fitting non-linear exposure-response relationships with Cox models in a simulation study," *International Journal of Biostatistics*, vol. 5, no. 1, 2009, doi: 10.2202/1557-4679.1104.

[64] D. Surya Prabha and J. Satheesh Kumar, "Performance analysis of image smoothing methods for low level of distortion," *2016 IEEE International Conference on Advances in Computer Applications, ICACA 2016*, pp. 372–376, 2017, doi: 10.1109/ICACA.2016.7887983.

[65] J. Kuruvilla and K. Gunavathi, "Lung cancer classification using neural networks for CT images," *Computer Methods and Programs in Biomedicine*, vol. 113, no. 1, pp. 202–209, 2014, doi: 10.1016/j.cmpb.2013.10.011.

[66] H. Zhu, F. H. Y. Chan, and F. K. Lam, "Image contrast enhancement by constrained local histogram equalization," *Computer Vision and Image Understanding*, vol. 73, no. 2, pp. 281–290, 1999, doi: 10.1006/cviu.1998.0723.

[67] P. Perona and J. Malik, "Scale-space and edge detection using anisotropic diffusion," *IEEE Transactions on Pattern Analysis and Machine Intelligence*, vol. 12, no. 7, pp. 629–639, 1990, doi: 10.1109/34.56205.

[68] A. E. Ilesanmi and T. O. Ilesanmi, "Methods for image denoising using convolutional neural network: A review," *Complex and Intelligent Systems*, vol. 7, no. 5, pp. 2179–2198, 2021, doi: 10.1007/s40747-021-00428-4.

[69] C. Anam *et al.*, "Noise reduction in CT images using a selective mean filter," *Journal of Biomedical Physics and Engineering*, vol. 10, no. 5, pp. 623–634, 2020, doi: 10.31661/jbpe.v0i0.2002-1072.

[70] A. Lucas, M. Iliadis, R. Molina, and A. K. Katsaggelos, "Using deep neural networks for inverse problems in imaging: Beyond analytical methods," *IEEE Signal Processing Magazine*, vol. 35, no. 1, pp. 20–36, 2018, doi: 10.1109/MSP.2017.2760358.

[71] A. Khan, A. Sohail, U. Zahoora, and A. S. Qureshi, "A survey of the recent architectures of deep convolutional neural networks," *Artificial Intelligence Review*, vol. 53, no. 8, pp. 5455–5516, 2020, doi: 10.1007/s10462-020-09825-6.

[72] Z. Guo, Y. Sun, M. Jian, and X. Zhang, "Deep residual network with sparse feedback for image restoration," *Applied Sciences (Switzerland)*, vol. 8, no. 12, 2018, doi: 10.3390/app8122417.

[73] C. Tian, L. Fei, W. Zheng, Y. Xu, W. Zuo, and C. W. Lin, "Deep learning on image denoising: An overview," *Neural Networks*, vol. 131, pp. 251–275, 2020, doi: 10.1016/j.neunet.2020.07.025.

[74] A. R. Pulagam, G. B. Kande, V. K. R. Ede, and B. R. Inampudi, "Automated lung segmentation from HRCT scans with diffuse parenchymal lung diseases," *Journal of Digital Imaging*, vol. 29, no. 4, pp. 507–519, 2016, doi: 10.1007/s10278-016-9875-z.

[75] E. M. Van Rikxoort, B. De Hoop, S. Van De Vorst, M. Prokop, and B. Van Ginneken, "Automatic segmentation of pulmonary segments from volumetric chest CT scans," *IEEE Transactions on Medical Imaging*, vol. 28, no. 4, pp. 621–630, 2009, doi: 10.1109/TMI.2008.2008968.

[76] Q. Wei, Y. Hu, G. Gelfand, and J. H. MacGregor, "Segmentation of lung lobes in high-resolution isotropic CT images," *IEEE Transactions on Biomedical Engineering*, vol. 56, no. 5, pp. 1383–1393, 2009, doi: 10.1109/TBME.2009.2014074.

[77] P. Campadelli, E. Casiraghi, and D. Artioli, "A fully automated method for lung nodule detection from postero-anterior chest radiographs," *IEEE Transactions on Medical Imaging*, vol. 25, no. 12, pp. 1588–1603, 2006, doi: 10.1109/TMI.2006.884198.

[78] D. C. Tseng and C. H. Chang, "Color segmentation using perceptual attributes," *Proceedings - International Conference on Pattern Recognition*, vol. 3, pp. 228–231, 1992, doi: 10.1109/ICPR.1992.201967.

[79] H. Da Cheng and Y. Sun, "A hierarchical approach to color image segmentation using homogeneity," *IEEE Transactions on Image*

Processing, vol. 9, no. 12, pp. 2071–2082, 2000, doi: 10.1109/83.887975.

[80] F. Spagnolo, S. Perri, and P. Corsonello, "An efficient hardware-oriented single-pass approach for connected component analysis," *Sensors (Switzerland)*, vol. 19, no. 14, 2019, doi: 10.3390/s19143055.

[81] A. Sheta, M. S. Braik, and S. Aljahdali, "Genetic algorithms: A tool for image segmentation," *Proceedings of 2012 International Conference on Multimedia Computing and Systems, ICMCS 2012*, pp. 84–90, 2012, doi: 10.1109/ICMCS.2012.6320144.

[82] A. Choudhury, R. R. Subramanian, and G. Sunder, "A novel approach for tumor segmentation for lung cancer using multi-objective genetic algorithm and connected component analysis," *Advances in Intelligent Systems and Computing*, vol. 828, pp. 367–376, 2019, doi: 10.1007/978-981-13-1610-4_37.

[83] J. R. F. da Silva Sousa, A. C. Silva, A. C. de Paiva, and R. A. Nunes, "Methodology for automatic detection of lung nodules in computerized tomography images," *Computer Methods and Programs in Biomedicine*, vol. 98, no. 1, pp. 1–14, 2010, doi: 10.1016/j.cmpb.2009.07.006.

[84] Y. Chunran and W. Yuanyuan, "Nodule on CT Images," pp. 2–6, 2018.

[85] T. Messay, R. C. Hardie, and T. R. Tuinstra, "Segmentation of pulmonary nodules in computed tomography using a regression neural network approach and its application to the lung image database consortium and image database resource initiative dataset," *Medical Image Analysis*, vol. 22, no. 1, pp. 48–62, 2015, doi: 10.1016/j.media.2015.02.002.

[86] S. P. Sankar and D. E. George, "Regression neural network segmentation approach with LIDC-IDRI for lung lesion," *Journal of Ambient Intelligence and Humanized Computing*, vol. 12, no. 5, pp. 5571–5580, 2021, doi: 10.1007/s12652-020-02069-w.

[87] H. Shaziya and K. Shyamala, "Pulmonary CT images segmentation using CNN and UNet models of deep learning," *2020 IEEE Pune Section International Conference, PuneCon 2020*, pp. 195–201, 2020, doi: 10.1109/PuneCon50868.2020.9362463.

[88] R. Arora, I. Saini, and N. Sood, "Modified UNet++ model: A deep model for automatic segmentation of lungs from chest X-ray images," *ICSCCC 2021 - International Conference on Secure Cyber Computing and Communications*, pp. 166–169, 2021, doi: 10.1109/ICSCCC51823.2021.9478101.

[89] K. L. Hua, C. H. Hsu, S. C. Hidayati, W. H. Cheng, and Y. J. Chen, "Computer-aided classification of lung nodules on computed tomography images via deep learning technique," *OncoTargets and Therapy*, vol. 8, pp. 2015–2022, 2015, doi: 10.2147/OTT.S80733.

[90] W. Ausawalaithong, A. Thirach, S. Marukatat, and T. Wilaiprasitporn, "Automatic lung cancer prediction from chest X-ray images using the deep learning approach," *BMEiCON 2018 - 11th Biomedical Engineering International Conference*, 2019, doi: 10.1109/BMEiCON.2018.8609997.

[91] D. Ardila *et al.*, "End-to-end lung cancer screening with three-dimensional deep learning on low-dose chest computed tomography," *Nature Medicine*, vol. 25, no. 6, pp. 954–961, 2019, doi: 10.1038/s41591-019-0447-x.

[92] I. Nazir, I. U. Haq, M. M. Khan, M. B. Qureshi, H. Ullah, and S. Butt, "Efficient pre-processing and segmentation for lung cancer detection using fused CT images," *Electronics (Switzerland)*, vol. 11, no. 1, 2022, doi: 10.3390/electronics11010034.

[93] M. Osadebey, H. K. Andersen, D. Waaler, K. Fossaa, A. C. T. Martinsen, and M. Pedersen, "Three-stage segmentation of lung region from CT images using deep neural networks," *BMC Medical Imaging*, vol. 21, no. 1, 2021, doi: 10.1186/s12880-021-00640-1.

[94] M. Chavan, V. Varadarajan, S. Gite, and K. Kotecha, "Deep neural network for lung image segmentation on chest X-ray," *Technologies*, vol. 10, no. 5, p. 105, 2022, doi: 10.3390/technologies10050105.

[95] R. Tandon, S. Agrawal, A. Chang, and S. S. Band, "VCNet: Hybrid deep learning model for detection and classification of lung carcinoma using chest radiographs," *Frontiers in Public Health*, vol. 10, 2022, doi: 10.3389/fpubh.2022.894920.

[96] Q. Wang, F. Shen, L. Shen, J. Huang, and W. Sheng, "Lung nodule detection in CT images using a raw patch-based convolutional neural network," *Journal of Digital Imaging*, vol. 32, no. 6, pp. 971–979, 2019, doi: 10.1007/s10278-019-00221-3.

[97] A. Masood *et al.*, "Automated decision support system for lung cancer detection and classification via enhanced RFCN with multilayer fusion RPN," *IEEE Transactions on Industrial Informatics*, vol. 16, no. 12, pp. 7791–7801, 2020, doi: 10.1109/TII.2020.2972918.

[98] S. Kido, Y. Hirano, and N. Hashimoto, "Detection and classification of lung abnormalities by use of convolutional neural network (CNN) and regions with CNN features (R-CNN)," *2018 International Workshop on Advanced Image Technology, IWAIT 2018*, pp. 1–4, 2018, doi: 10.1109/IWAIT.2018.8369798.

[99] Q. Dou, H. Chen, L. Yu, J. Qin, and P. A. Heng, "Multilevel contextual 3-D CNNs for false positive reduction in pulmonary nodule detection," *IEEE Transactions on Biomedical Engineering*, vol. 64, no. 7, pp. 1558–1567, 2017, doi: 10.1109/TBME.2016.2613502.

[100] M. Anthimopoulos, S. Christodoulidis, L. Ebner, A. Christe, and S. Mougiakakou, "Lung pattern classification for interstitial lung diseases using a deep convolutional neural network," *IEEE Transactions on Medical Imaging*, vol. 35, no. 5, pp. 1207–1216, 2016, doi: 10.1109/TMI.2016.2535865.

[101] R. Bhakkiyalakshmi, P. Ponnammal, M. K. Srilekha, and K. Abhishikt Sai, "Fast and adaptive detection of pulmonary nodules in thoracic CT images using a contextual clustering based region growing," *International Journal of Engineering and Technology(UAE)*, vol. 7, no. 2, pp. 106–108, 2018, doi: 10.14419/ijet.v7i2.24.12010.

[102] L. Böröczky, L. Zhao, and K. P. Lee, "Feature subset selection for improving the performance of false positive reduction in lung nodule CAD," *IEEE Transactions on Information Technology in Biomedicine*, vol. 10, no. 3, pp. 504–511, 2006, doi: 10.1109/TITB.2006.872063.

[103] T. Jia, D. Z. Zhao, Y. Wei, X. H. Zhu, and X. Wang, "Computer-aided lung nodule detection based on CT images," *2007 IEEE/ICME International Conference on Complex Medical Engineering, CME 2007*, pp. 816–819, 2007, doi: 10.1109/ICCME.2007.4381854.

[104] A. R. Talebpour, H. R. Hemmati, and M. Z. Hosseinian, "Automatic lung nodules detection in computed tomography images using nodule filtering and neural networks," *22nd Iranian Conference on Electrical Engineering, ICEE 2014*, pp. 1883–1887, 2014, doi: 10.1109/IranianCEE.2014.6999847.

[105] R. Golan, C. Jacob, and J. Denzinger, "Lung nodule detection in CT images using deep convolutional neural networks," *Proceedings of the International Joint Conference on Neural Networks*, vol. 2016-October, pp. 243–250, 2016, doi: 10.1109/IJCNN.2016.7727205.

[106] H. Shi, Z. Peng, and H. Wan, "Pulmonary nodules detection based on CNN multi-scale feature fusion," *2019 IEEE 11th International Conference on Advanced Infocomm Technology, ICAIT 2019*, pp. 86–90, 2019, doi: 10.1109/ICAIT.2019.8935936.

BIOGRAPHIES OF AUTHORS

Sekar Sari received her B.Eng. degree in Electrical Engineering from Universitas Ahmad Dahlan, Yogyakarta, Indonesia, in 2019. After graduating, she pursued a Master's degree in the Department of Electrical and Information Engineering at Universitas Gadjah Mada, Indonesia, and received her M.Eng. in 2022. Her research interests include electronics design, deep learning, biomedical engineering, image processing, and pattern recognition. She can be contacted at sekarsari103@gmail.com.

Tole Sutikno is a lecturer in the Electrical Engineering Department at the Universitas Ahmad Dahlan (UAD), Yogyakarta, Indonesia. He received his B.Eng., M.Eng., and Ph.D. degrees in Electrical Engineering from Universitas Diponegoro, Universitas Gadjah Mada, and Universiti Teknologi Malaysia, in 1999, 2004, and 2016, respectively. He has been an Associate Professor at UAD, Yogyakarta, Indonesia since 2008. He is currently the Editor-in-Chief of the Bulletin of Electrical Engineering and Informatics and the Head of the Embedded Systems and Power Electronics Research Group. His research interests include the fields of digital design, industrial applications, industrial electronics, industrial informatics, power electronics, motor drives, renewable energy, FPGA applications, embedded systems, artificial intelligence, intelligent systems, image processing, information systems, and digital libraries. He can be contacted by email at tole@ee.uad.ac.id.

Indah Soesanti received the M.Eng. and Ph.D. degrees from the Department of Electrical Engineering, Universitas Gadjah Mada, Yogyakarta, Indonesia. She is currently a Lecturer with the Department of Electrical and Information Engineering, Faculty of Engineering, Universitas Gadjah Mada. Her research interests include artificial intelligence, optimization, signal processing, image processing, information systems, ICT-based systems, biomedical engineering, and pattern classification. She can be contacted at indahsoesanti@ugm.ac.id.

Noor Akhmad Setiawan received his Bachelor and Master degree in Electrical Engineering from Universitas Gadjah Mada in 1998 and 2003 respectively. He received his PhD degree in Electrical and Electronics Engineering from Universiti Teknologi PETRONAS in 2009. He is with the Department of Electrical and Information Engineering Universitas Gadjah Mada. His research interest includes machine learning, soft computing, data mining, big data, medical engineering and informatics, and electrical engineering. He is a member of IEEE, ACM, IRSS, IAENG and IACSIT. He can be contacted by email at noorwewe@ugm.ac.id.